Acta Physiologica Sinica, February 25, 2014, 66(1): 85–95
DOI: 10.13294/j.aps.2014.0011 http://www.actaps.com.cn

Research Paper

Ionic mechanism underlying distinctive excitability in atrium and ventricle of the heart

Hai-Ying Sun[1], Guo-Sheng Xiao[2], Yan Wang[2], Gui-Rong Li[1,*]

[1]*Departments of Physiology and Medicine, Li Ka Shing Faculty of Medicine, The University of Hong Kong, Hong Kong, China;* [2]*Xiamen Heart Center, Zhongshan Hospital, Medical School of Xiamen University, Xiamen 361004, China*

Abstract: Cellular excitability is an important physiological factor in maintaining normal cardiac activity. The present study was designed to investigate the ionic mechanism underlying different excitability in atrial and ventricular myocytes of guinea pig heart using a whole-cell patch configuration. We found that excitability is lower in ventricular myocytes than that in atrial myocytes. Although the density of voltage-gated fast Na^+ current (I_{Na}) was lower in ventricular myocytes, it would not correlate to the lower excitability since its availability was greater than that in atrial myocytes around threshold potential. Classical inward rectifier K^+ current (I_{K1}) was greater in ventricular myocytes than that in atrial myocytes, which might contribute in part to the lower excitability. In addition, the transient outward K^+ current with inward rectification (I_{toir}) elicited by depolarization was greater in ventricular myocytes than that in atrial myocytes and might contribute to the lower excitability. In ventricular myocytes, Ba^{2+} at 5 μmol/L significantly inhibited I_{toir}, enhanced excitability, and shifted the threshold potential of I_{Na} activation to more negative, and the effect was independent of affecting I_{Na}. Our results demonstrate the novel information that in addition to classical I_{K1}, I_{toir} plays a major role in determining the distinctive excitability in guinea pig atrial and ventricular myocytes and maintaining cardiac excitability. More effort is required to investigate whether increase of I_{toir} would be protective via reducing excitability.

Key words: cardiac electrophysiology; whole-cell patch clamp; excitability; transient outward K^+ current with inward rectification; inward rectifier K^+ current; voltage-gated Na^+ current

心房与心室肌细胞兴奋性不同的离子机理研究

孙海英[1]，肖国胜[2]，王 焱[2]，李贵荣[1,*]

[1]香港大学李嘉诚医学院生理学系和内科学系，香港；[2]厦门大学医学院，中山医院，厦门心脏中心，厦门 361004

摘 要：心肌细胞兴奋性是维持正常的心脏活动的一个重要生理因素。本研究旨在使用全细胞膜片技术探讨豚鼠心房和心室肌细胞不同兴奋性的离子机理。结果显示，心室肌细胞兴奋性比心房肌细胞低。虽然豚鼠心室肌细胞的电压门控快Na^+电流(I_{Na})密度较低，但与其兴奋性较低并不相关，因为其在阀电位附近的可用度比率比心房肌细胞高。经典内向整流钾电流(I_{K1})在心室肌细胞比在心房肌细胞更大，这可能是心室肌细胞兴奋性较低的部分原因。此外，去极化引起的有内向整流特性的瞬时外向钾电流(I_{toir})在心室肌细胞较大，并可能是其兴奋性较低的主要原因。在心室肌细胞，5 μmol/L Ba^{2+}显著抑制I_{toir}，增强细胞兴奋性，并使I_{Na}激活的阈电位更负，其作用独立于对I_{Na}的影响。本研究结果证明，除经典的I_{K1}外，I_{toir}在豚鼠心房肌和心室肌细胞的兴奋性差异形成和心肌兴奋性维持中起着主要作用。然而，I_{toir}增加是否会通过降低兴奋性以保护心脏，还需要进一步研究。

关键词：心脏电生理学；全细胞膜片钳技术；兴奋性；内向整流性瞬时外向钾电流；内向整流钾电流；电压门控钠离子电流

中图分类号：R331.3+8

This work was supported by Sun Chieh Yeh Heart Foundation of Hong Kong and a General Research Fund (HKU 771712M) from Research Grant Council of Hong Kong.

*Corresponding author. Tel: +852-28199513; E-mail: grli@hkucc.hku.hk

Cardiac excitability is defined as "the ease with which cardiac cells undergo a series of events with characterization of the sequential depolarization and repolarization, the communication with adjacent cells, and the propagation of the electrical activity in a normal or abnormal manner" [1]. As in other excitable tissues/cells [2–4], cardiac excitability can be evaluated by the strength-duration curve [5–9]. It is believed that cardiac excitability is determined by the difference between the threshold membrane potential and the resting membrane potential [10]. Nonetheless, both the threshold membrane potential and resting membrane potential are determined by different ion channels, e.g. K^+ channels [11] and/or Na^+ channels [10]. An earlier study demonstrated that cellular excitability was greater in atrial myocytes than that in ventricular myocytes from rabbit hearts, which is believed to be contributed by differential inward rectifier K^+ current (I_{K1}), i.e. greater I_{K1} in ventricular myocytes [12]. We previously found that the greater density of voltage-gated Na^+ current (I_{Na}) likely also contributes to the higher excitability in guinea pig atrial myocytes [13].

It was generally recognized that the cardiac I_{K1} channels are the heterotetrameric assembly of different Kir2 subfamily members, including Kir2.1, Kir2.2 and Kir2.3 [14]. Cardiac I_{K1} channel was considered to act as a diode [15] that activates only on hyperpolarization of the membrane [16], and very little current passing through the channel in the outward direction during membrane depolarization under physiological conditions [15, 16]; and therefore I_{K1} was thought to be inactivated during the upstroke and plateau phases of the action potential and is consequently available for repolarization only during phase 3 [17]. However, our experimental studies have demonstrated a transient outward K^+ current with inward rectification (I_{toir}) activated by depolarization is an important component of I_{K1} in canine ventricular myocytes [18] and guinea pig atrial and ventricular myocytes [19], which has been further confirmed in HEK 293 cells stably expressing Kir2.1 channels [20, 21]. The significant outward current carried by I_{toir} can be elicited by depolarization at very negative potentials over a time course comparable to I_{Na}, which implies an important contribution to cellular excitability [18–21]. The present study was designed to investigate whether distinctive excitability would present in guinea pig heart, and whether I_{toir} contributes to the differential excitability in atrial and ventricular myocytes of guinea pig heart.

1 MATERIALS AND METHODS

1.1 *Cell preparation*

Single atrial and ventricular myocytes were prepared with guinea pig hearts using a modified procedure described previously [13]. The experimental protocol was approved by the Committee on the Use of Live Animals in Teaching and Research of the University of Hong Kong. Briefly, after guinea pigs (300–350 g, either gender) were anesthetized with phenobarbital (30–40 mg/kg i.p.), their hearts were quickly removed and placed in oxygenated Tyrode's solution. The heart was mounted on a Langendorf column, and initially perfused with oxygenated Tyrode's solution (37 °C) for cleaning blood (about 5 min). After the heart was superfused with Ca^{2+}-free Tyrode's solution for 8–10 min, it was enzymatically digested with a solution containing 0.06% collagenase (Type II, Worthington Biochemical) and 0.1% bovine serum albumin (Sigma) until the heart was softened. The left atrium and/or ventricle were then excised from the softened heart, placed in a high-K^+ storage medium (see 1.2 Solutions). A small aliquot of the solution containing the isolated cells was placed in an open perfusion chamber (1 mL) mounted on the stage of an inverted microscope. Experiments were conducted at room temperature (22–23 °C) for current recording in voltage-clamp mode, while at 37 °C for action potential recording and excitability determination in current-clamp mode. Only quiescent rod-shaped cells showing clear cross-striations were used.

1.2 *Solutions*

Tyrode's solution contained (mmol/L): 136 NaCl, 5.4 KCl, 1 $MgCl_2$, 2 $CaCl_2$, 0.33 NaH_2PO_4, 10 glucose and 10 HEPES; pH adjusted to 7.4 with NaOH. When I_{Na} was eliminated, NaCl in Tyrode's solution was replaced by equimolar choline chloride. The pipette solution contained (mmol/L): 20 KCl, 110 K-aspartate, 1 $MgCl_2$, 10 HEPES, 5 EGTA, 0.1 GTP, 5 Mg_2ATP, 3 Na_2-phosphocreatine; pH adjusted to 7.2 with KOH. When I_{Na} was recorded, symmetrical Na^+ (5 mmol/L) was used in pipette and bath solution, K^+ and Na^+ were replaced by equimolar Cs^+. The high K^+-storage medium contained (mmol/L): 20 KCl, 10 KH_2PO_4, 70 K-glutamate, 20 taurine, 10 β-hydroxybutyric acid, 25 glucose, 20 mannitol, 0.5 EGTA, as well as 0.1% albumin, with pH adjusted to 7.2 with KOH. $CdCl_2$ (100 μmol/L) was used to block Ca^{2+} current (I_{Ca}), and atropine (1 μmol/L) was used to block possible muscarinic receptor-mediated

current.

1.3 *Electrophysiology and data analysis*

The whole-cell patch-clamp technique was used for electrophysiological recording. Borosilicate glass electrodes (1.2-mm OD) were pulled with a Brown-Flamming puller (model P-97, Sutter Instrument Co., Novato, CA., UAS) and had tip resistances of 2–3 MΩ, when filled with pipette solution. Membrane currents were recorded using an EPC-9 amplifier and Pulse software (HEKA, Lambrecht, Germany). A 3-M KCl-agar salt bridge was used as reference electrode, and tip potentials were compensated before the pipette touched the cell. After a gigaohm seal was obtained, the cell membrane was ruptured by gentle suction to establish the whole-cell configuration. Junction potentials (12–15 mV) between pipette solution and bath solution were not justified. The cell membrane capacitance was directly measured using the lock-in module of the Pulse software, and used for normalizing the current in individual cells. The series resistance (2–5 MΩ) was compensated by 60%–80% to minimize voltage errors. Signals were low-pass filtered at 5 kHz and stored on the hard disk of an IBM compatible computer.

1.4 *Statistical analysis*

Nonlinear curve fitting was performed using Pulsefit (HEKA) and Sigmaplot (SPSS, Chicago, IL). Paired and/or unpaired Student's *t*-test was used as appropriate to evaluate the statistical significance of differences between two group means, and ANOVA was used for multiple groups. Values of $P < 0.05$ were considered to indicate statistical significance. Results are presented as mean ± S.E.M.

2 RESULTS

2.1 Action potentials and cellular excitability in guinea pig ventricular and atrial myocytes

Action potentials were recorded at 37 °C in current-clamp mode in atrial and ventricular myocytes. Figure 1*A* illustrates the representative action potentials recorded (1 Hz) in an atrial cell (left) and a ventricular cell (right). Action potential duration (APD) was shorter in atrial cell than that in ventricular cell, while resting membrane potential was slightly positive in the atrial cell. Resting membrane potential and APD at 90% repolarization (APD90) were (–62.9 ± 2.1) mV and (127 ± 9.7) ms in atrial cells ($n = 17$), and (–69.3 ± 1.8) mV and (174.7 ± 11.4) ms in ventricular cells ($n = 25$, $P < 0.01$ *vs* atrial cells). These results suggested that action potential characterization differs in atrial myocytes from that in ventricular myocytes.

To determine whether the differential excitability would also present in guinea pig hearts, cell excitability was evaluated in atrial and ventricular myocytes by determining strength-duration relation curve as described previously [12, 22]. The minimal current strength was determined with variable current duration (0.5, 1, 3, 5, 10, and 50 ms), and plotted against the duration. The frequency of determining the strength-duration relation curve was low at 0.2 Hz to allow full recovery of excitability during diastole. Figure 1*B* shows the strength-duration relation curves determined in atrial and ventricular myocytes. More current was

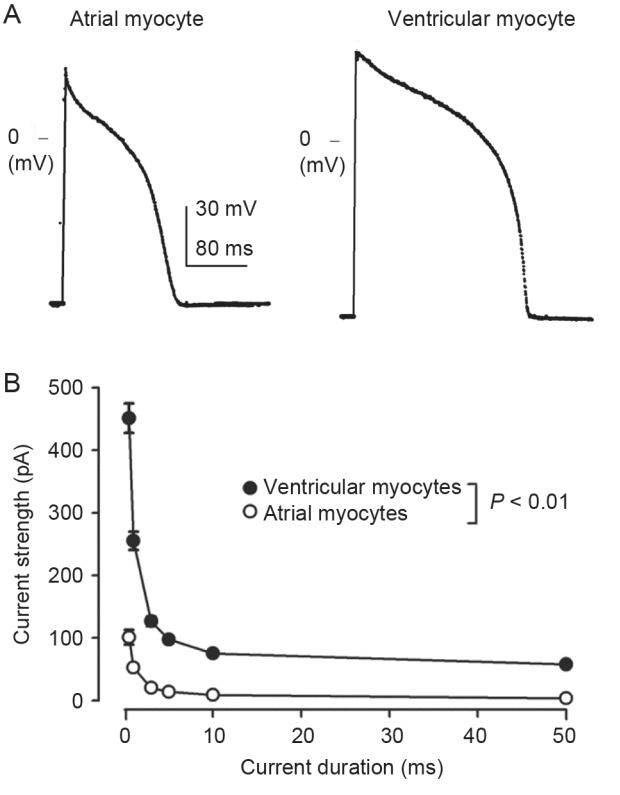

Fig. 1. Action potentials and current strength-duration relationship curves in guinea pig atrial and ventricular myocytes. *A*: Representative action potentials recorded in an atrial myocyte (left panel) and a ventricular myocyte (right panel) in current-clamp mode (1 Hz). *B*: Current strength-duration relationship curves determined at consistent membrane potential of −80 mV by the minimal current strength to trigger action potential in guinea pig atrial myocytes ($n = 12$) and ventricular myocytes ($n = 11$, $P < 0.01$ *vs* atrial myocytes). The current strength values were plotted against variable (0.5, 1, 3, 5, 10, and 50 ms) current duration.

required to triggering action potential at short durations of current step. The current required for triggering action potentials was greater in ventricular myocytes (n = 11) than that in atrial myocytes (n = 12) for each current step duration ($P < 0.01$), suggesting that excitability is lower in ventricular myocytes than that in atrial myocytes of guinea pig heart, similar to that in rabbit heart [12].

To investigate whether the differential excitability would be resulted from the different resting membrane potential in atrial and ventricular myocytes, we determined the threshold potential by keeping the membrane potential at −80 mV in both atrial and ventricular myocytes using a 50-ms current step with variable current amplitudes. Figure 2*A* illustrates the representative recordings for determining the threshold potential in an atrial myocyte and a ventricular myocyte. The threshold potential for generating action potential was −53 mV with 32 pA in the atrial myocyte, while was −42 mV with 61 pA in the ventricular myocyte. The mean value of threshold potential (Fig. 2*B*) was (–52.6 ± 2.7) mV in atrial myocytes (n = 12), and (–41.8 ± 1.5) mV in ventricular myocytes (n = 13, $P < 0.01$ *vs* atrial myocytes). These results suggest that lower excitability is not mainly related to the more negative resting membrane potential in ventricular myocytes, which may be resulted from the different ion channels (I_{Na}, classical I_{K1}, and/or I_{toir}) which would determinate the excitability. The following experiments will analyze whether and how I_{Na}, classical I_{K1}, and/or I_{toir} contribute to the distinctive difference of excitability in atrial and ventricular myocytes.

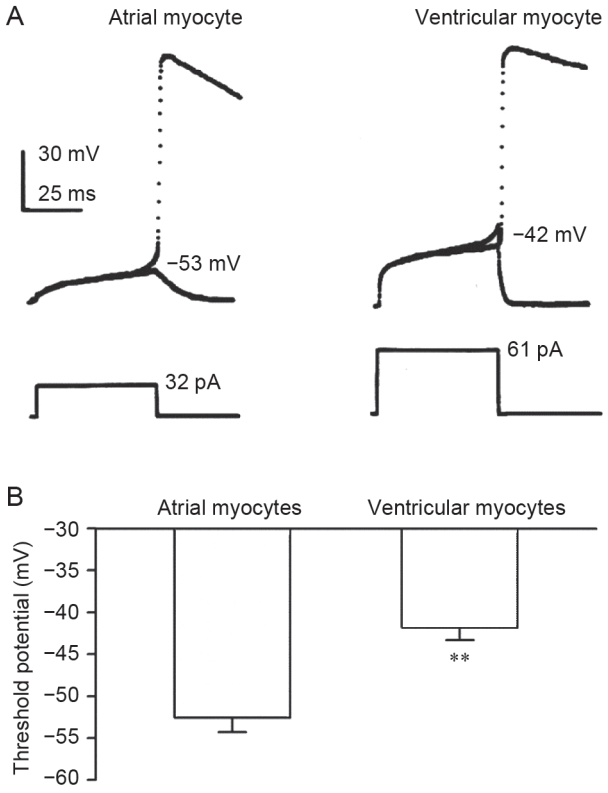

Fig. 2. Threshold potential of action potential activation in guinea pig atrial and ventricular myocytes. *A*: Measurement of threshold potential for triggering action potential using 50 ms current duration in an atrial myocyte (left panel) and a ventricular myocyte (right panel) with the current strength amplitude shown. *B*: Mean values of threshold potential for action potential generation in atrial (n = 12) and ventricular myocytes (n = 13, $^{**}P < 0.01$ *vs* atrial myocytes).

2.2 Potential contribution of cardiac I_{Na} to the differential excitability

Our previous study has demonstrated that in addition to the different biophysical properties of I_{Na} in atrial and ventricular myocytes of guinea pig hearts, the density of I_{Na} is greater in atrial myocytes than that in ventricular myocytes [13]. To determine whether the lower excitability is related to the less density of I_{Na} in ventricular myocytes, we recorded I_{Na} here in atrial and ventricular myocytes. Figure 3*A* shows the representative I_{Na} traces recorded in an atrial (left) and a ventricular (right) myocytes. The activation and inactivation of I_{Na} was slower in ventricular myocytes than those in atrial myocytes (n = 15), while the current density (Fig. 3*B*) was greater in atrial myocytes than that in ventricular myocytes (n = 12, $P < 0.05$ or $P < 0.01$ *vs* atrial myocytes), and the threshold potential of I_{Na} was more negative in atrial myocytes than that in ventricular myocytes ($P < 0.05$), which might imply the potential contribution of I_{Na} to higher excitability in atrial myocytes. However, potential of I_{Na} availability was more positive in ventricular myocytes than that in atrial myocytes, indicating that more Na^+ channels in ventricular myocytes are available to open around threshold potentials (Fig. 3*C*). Therefore, it is postulated that the potential contribution of I_{Na} to the distinctive excitability in atrial and ventricular myocytes is limited.

2.3 Potential contribution of cardiac classical I_{K1} and I_{toir} to the differential excitability

It is generally recognized that classical I_{K1} plays an important role in stabilizing membrane potential in the heart [23, 24], and density of I_{K1} is greater in ventricular myocytes than that in atrial myocytes [19, 21]. Here, we also determined classical I_{K1} in guinea pig atrial and

ventricular myocytes (Fig. 4) with the voltage protocol: 300-ms voltage steps between −100 and −20 mV from a holding potential of −40 mV. Figure 4*A* shows the representative I_{K1} traces recorded from an atrial myocyte and a ventricular myocyte. Amplitude of I_{K1} was smaller in the atrial cell than that in the ventricular cell. Interestingly, the *I–V* relationship curves of mean I_{K1} amplitude (left panel) and current density (right panel) showed a large outward component with strong inward rectification and greater density in ventricular myocytes, while a small outward component and less density in atrial myocytes. The higher density of I_{K1} clearly correlates to the relative more negative resting membrane potential of action potentials in ventricular myocytes, and may also contribute to at least in part to the lower excitability. However, it was believed that I_{K1} was inactivated on depolarization, and activated on repolarization [15–17]. Therefore, contribution of classical I_{K1} to the different excitability may be limited in atrial and ventricular myocytes.

I_{toir} is the current that was previously ignored component of I_{K1} activated by depolarization [19–21], which may be important in determining the distinctive excitability. We therefore measured I_{toir} in atrial and ventricular myocytes in Na^+-free Tyrode's solution with the same procedure as described previously [19] to limit the contamination of I_{Na}. Figure 5*A* shows the representative I_{toir} traces recoded in an atrial myocyte and a ventricular myocyte with 300-ms depolarization steps between −70 and 0 mV from a holding potential of −80 mV. Amplitude of I_{toir} was significantly larger in the ventricular

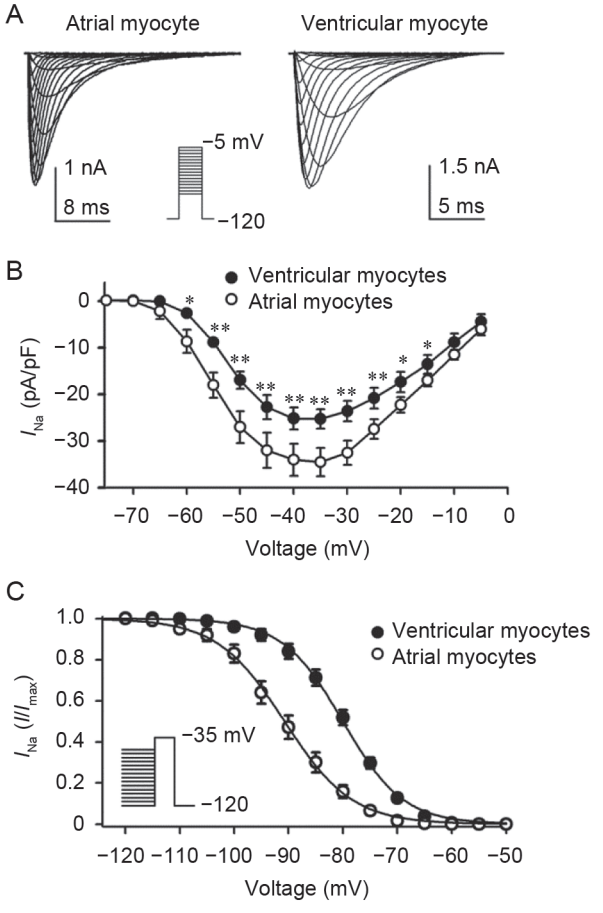

Fig. 3. Voltage-gated I_{Na} in guinea pig atrial and ventricular myocytes. *A*: Representative I_{Na} traces recorded in an atrial myocyte (left panel) and a ventricular myocyte (right panel) with the voltage protocol shown. *B*: *I–V* relationship curves of I_{Na} density in atrial (n = 15) and ventricular myocytes (n = 12, $^*P < 0.05$, $^{**}P < 0.01$ *vs* atrial myocytes). *C*: Mean values of variables of I_{Na} availability were fitted to a Boltzmann function as described previously [13]. The V0.5 of I_{Na} availability was (−80.1 ± 2.3) mV in ventricular myocytes (n = 12), while (−90.7 ± 1.5) mV in atrial myocytes (n = 15, $P < 0.01$ *vs* ventricular myocytes).

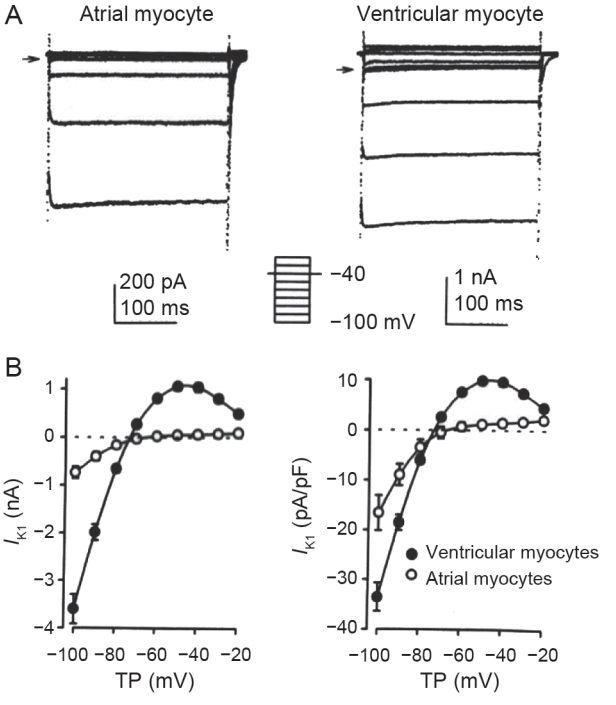

Fig. 4. Classical inward rectifier K^+ current (I_{K1}) in guinea pig atrial and ventricular myocytes. *A*: Representative I_{K1} traces recorded with 300-ms voltage steps between −100 and −20 mV from a holding potential of −40 mV in an atrial myocyte (left panel) and a ventricular myocyte (right panel). *B*: *I–V* relationship curves of I_{K1} amplitude (left panel) and density (right panel) in atrial myocytes (n = 10) and ventricular myocytes (n = 9). The current amplitude and density were greater in ventricular myocytes ($P < 0.05$ or $P < 0.01$ *vs* atrial myocytes) than those in atrial myocytes at all test potentials (TP).

cell than that in the atrial cell. *I–V* relationships of the mean peak current measured from the current peak to the steady-state level are illustrated in Fig. 5*B*. Density of I_{toir} was significantly greater in ventricular myocytes (n = 12) than that in atrial myocytes (n = 11) at test potentials from −60 to +40 mV ($P < 0.05$ or $P < 0.01$). We have demonstrated that I_{toir} is carried by Kir2.x channels[20, 21]. This component of I_{K1} was ignored previously for several decades with holding potential of −40 mV, at which I_{toir} was inactivated significantly [18–20]. I_{toir} is elicited by depolarization at very negative potentials over a time course comparable to I_{Na} [18–20]. Therefore, I_{toir} likely plays a major role in determining excitability and is related to the distinctive excitability of atrial and ventricular myocytes.

2.4 I_{toir} inhibition and cardiac excitability

It is recognized that I_{K1} and Kir2.x are sensitive to inhibition by Ba^{2+} [20, 25, 26]. We previously found that I_{toir} was also sensitive to inhibition by Ba^{2+} [18–20], and therefore determined the effects of low concentrations of Ba^{2+} on action potential, cell excitability, threshold potential for I_{Na} activation in guinea pig ventricular myocytes. APD90 (APD at 90% repolarization) was increased by 5 μmol/L Ba^{2+} from (172.7 ± 9.9) ms of control (1 Hz) to (199.4 ± 17.1) ms (n = 10, $P < 0.01$ *vs* control), while resting membrane potential was decreased from (–70.9 ± 0.4) mV of control to (−69.6 ± 0.6) mV ($P < 0.05$ *vs* control), suggesting an inhibition of classical I_{K1}.

Figure 6*A* shows the representative I_{toir} traces in a ventricular myocyte recorded with 300-ms voltage steps between −70 to +60 mV from a holding potential of −80 mV in the absence (control) and presence of 5 μmol/L Ba^{2+}. Ba^{2+} inhibited both I_{toir} and steady-state (classical) component of I_{K1} channels. Figure 6*B* displays the *I–V* relationship curves of mean density of I_{toir} in guinea pig ventricular myocytes. Ba^{2+} (5 μmol/L) significantly reduced the current at test potentials of −60 to +60 mV (n = 11, $P < 0.01$ *vs* control), suggesting the inhibition of I_{toir} may result in an increase of myocytes excitability.

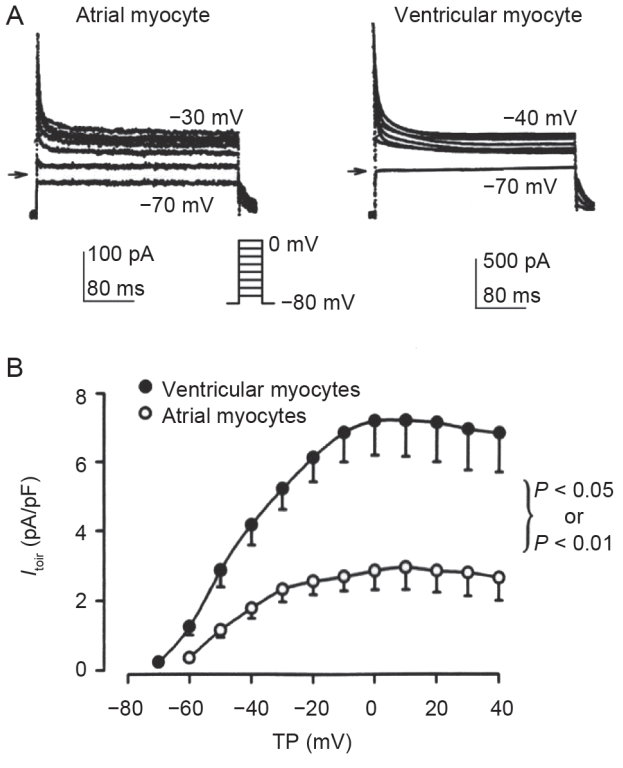

Fig. 5. Transient outward K^+ current with inward rectification (I_{toir}) in guinea pig atrial and ventricular myocytes. *A*: I_{toir} recorded with the voltage protocol shown in the inset in an atrial myocyte and a ventricular myocyte. *B*: *I–V* relationship curves of I_{toir} density in atrial (n = 11) and ventricular myocytes (n = 12).

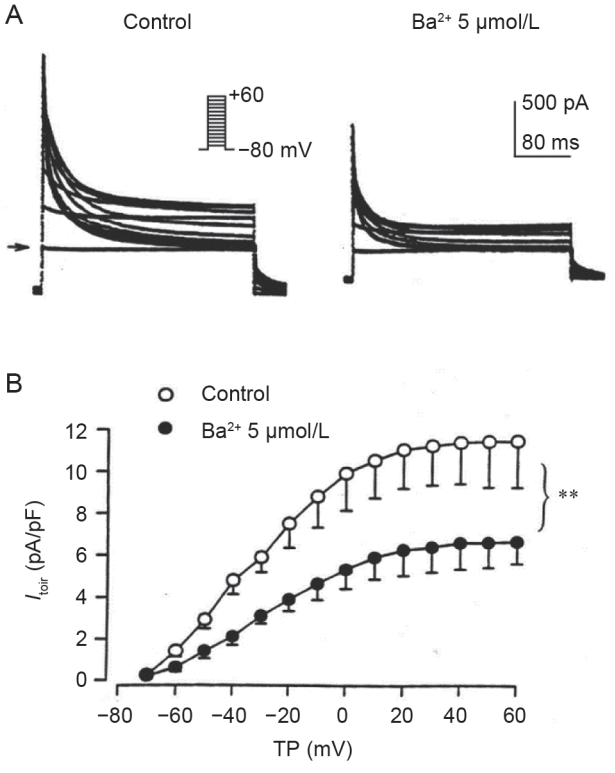

Fig. 6. Effect of Ba^{2+} on I_{toir} in guinea pig ventricular myocytes. *A*: I_{toir} tracings recorded from a representative ventricular cell in the absence (control) and presence of 5 μmol/L Ba^{2+} with the protocol shown in the inset. *B*: *I–V* relationship curves of I_{toir} in the absence and presence of 5 μmol/L Ba^{2+} (n = 11, $^{**}P < 0.01$ *vs* control).

Figure 7A shows the current strength-duration relation curves determined with consistent membrane potential of −80 mV in ventricular myocytes in the absence and presence of 5 μmol/L Ba^{2+} in current-clamp mode. Ba^{2+} slightly, but significantly shifted the curve to the left-downward (n = 12, $P < 0.01$ *vs* control), implying an increase of excitability. The calculated cell excitability at 5-ms current duration was increased by Ba^{2+} (0.5–10 μmol/L) in a concentration-dependent manner (n = 12, $P < 0.05$ or $P < 0.01$ *vs* control) (Fig. 7*B*). These results suggest that the increase of excitability may be related to inhibition of I_{toir} in ventricular myocytes.

To investigate how the excitability is increased by inhibiting I_{toir}, threshold potential of I_{Na} activation was determined in voltage-clamp mode. Figure 8*A* illustrates the representative current traces activated by voltage-steps from a holding potential of −80 mV in a ventricular myocyte in the absence and presence of 5 μmol/L Ba^{2+}. The threshold potential of I_{Na} activation was −44 mV before Ba^{2+} (control) with large I_{toir}, and −48 mV after application of Ba^{2+} with reduced I_{toir}. Figure 8*B* shows the mean values of the threshold potential of I_{Na} activation in the absence and presence of 1, 5, 10 μmol/L Ba^{2+}. The threshold potential was reduced by Ba^{2+} in a concentration-dependent manner. These results indicate that the increase of cell excitability by Ba^{2+} is related to reducing threshold potential of I_{Na} activation via inhibiting I_{toir}.

However, the potential involvement of I_{Na} increase should be excluded for the increased cell excitability by Ba^{2+}. We therefore determined the effect of Ba^{2+} on I_{Na}

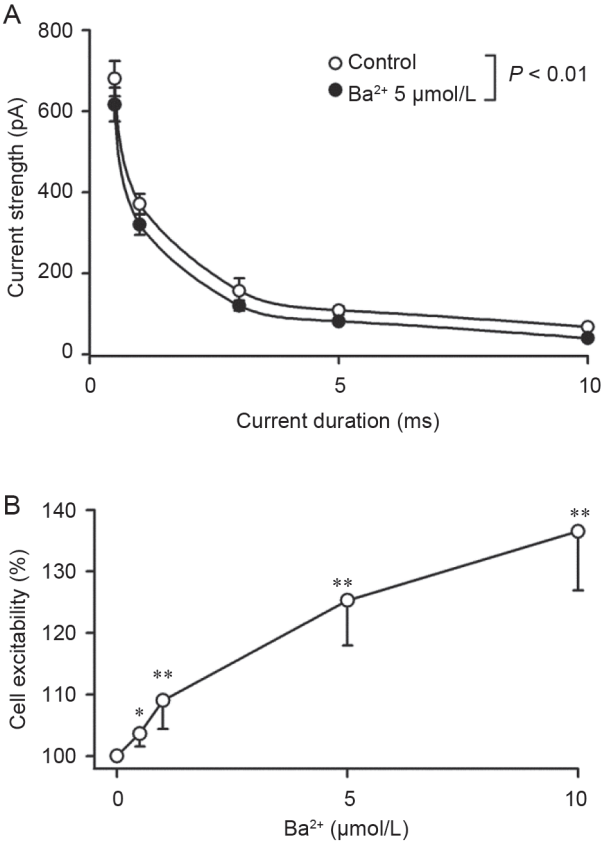

Fig. 7. Effect of Ba^{2+} on cell excitability at the constant membrane potential of −80 mV in guinea pig ventricular myocytes. *A*: Strength-duration curves before (control) and after application of 5 μmol/L Ba^{2+}. Ba^{2+} shifted the curve to the left-downward. *B*: Percentage (excitability) of change in the current threshold strength (with 5 ms current) by Ba^{2+} in a concentration-dependent manner (n = 12, $^{*}P < 0.05$, $^{**}P < 0.01$ *vs* control).

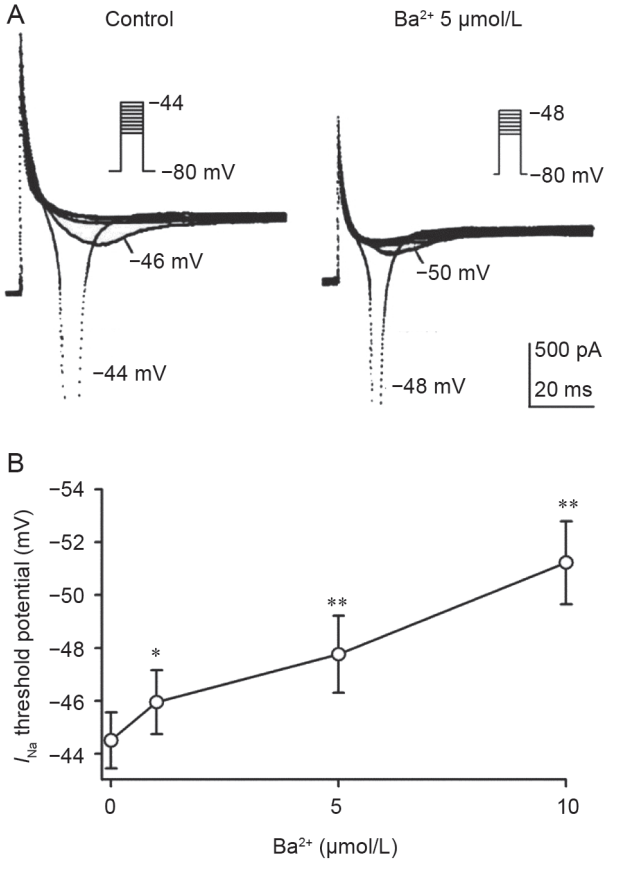

Fig. 8. Effect of Ba^{2+} on the threshold potential of I_{Na} activation in guinea pig ventricular myocytes. The membrane currents were recorded in Tyrode's solution with the voltage steps as shown in the insets. *A*: Current tracings were recorded in the absence (control) and presence of 5 μmol/L Ba^{2+} in a representative cell. *B*: Mean values of threshold potential for I_{Na} activation in the absence and present of 1, 5, and 10 μmol/L Ba^{2+}, showing concentration-dependent effect of Ba^{2+} on I_{Na} threshold potential (n = 10, $^{*}P < 0.05$, $^{**}P < 0.01$ *vs* control).

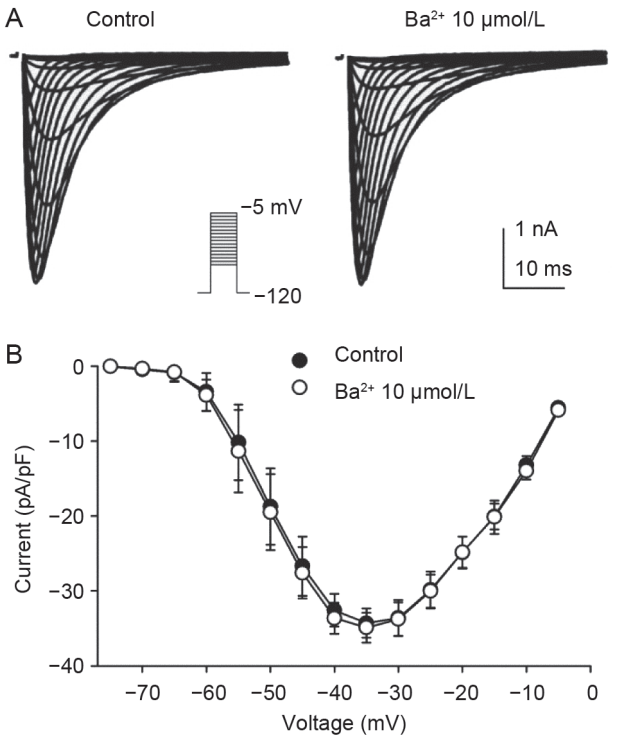

Fig. 9. Effect of Ba^{2+} on I_{Na} in guinea pig ventricular myocytes. *A*: Representative I_{Na} tracings recorded from a guinea pig ventricular cell in the absence (control) and presence of 10 μmol/L Ba^{2+}. *B*: *I–V* relationship curves of I_{Na} in the absence (control) and presence of 10 μmol/L Ba^{2+} (n = 7, P = NS).

in guinea pig ventricular myocytes. Figure 9*A* illustrates the representative I_{Na} traces recorded with protocol as shown in the inset in a ventricular myocyte in the absence and presence of Ba^{2+}. I_{Na} was not affected by application of 10 μmol/L Ba^{2+}. *I–V* relationship curve of mean I_{Na} density was not affected by Ba^{2+}, either (Fig. 9*B*). This result indicates that I_{Na} is not involved in the increase of cell excitability by Ba^{2+}.

3 DISCUSSION

In the present study, we have demonstrated that excitability is lower in ventricular myocytes than that in atrial myocytes of guinea pig heart. Although the density of I_{Na} is less in ventricular myocytes, but its contribution to the lower excitability is limited due to the higher availability of the channels around threshold potential. Classical component of I_{K1} activated during repolarization and I_{toir} activated during depolarization are significantly greater in ventricular myocytes, which likely contribute to the distinctive excitability in guinea pig atrial and ventricular myocytes. Ba^{2+} at low concentrations significantly increases the excitability in ventricular myocytes by reducing the threshold potential of I_{Na} activation via inhibiting I_{toir}. Therefore, I_{toir} likely plays an important role in the early repolarization of action potential and in maintaining cardiac excitability.

Although it is customary to consider that excitability is largely controlled by I_{Na}, experimental studies have demonstrated that the excitability in intact cells can be influenced by other membrane currents including I_{K1} [11, 27], and ATP-sensitive current (I_{KATP}) [28, 29] which can act as modulators of cell excitability during myocardial ischemia. Under normal conditions interplay between I_{K1} and the rapid I_{Na} is a major factor in controlling cardiac excitability [30]. The present results and the report from others [12] demonstrated that excitability was lower in ventricular myocytes than that in atrial myocytes. The difference of excitability in these two types of cells is believed to play important physiological roles in allowing the atrial cells to be driven easily by normal regions of automaticity (e.g., the sinoatrial node), the ventricular cells to prevent electrical initiation from other region of automaticity (e.g., an ectopic focus) [12]. The difference may be resulted from the distinctive distribution of inward I_{Na} and outward K^+ currents (e.g. I_{toir} activated by depolarization and classical I_{K1} activated by repolarization).

The greater density of I_{Na} in atrial myocytes [13] may correlate to the higher excitability. However, the less availability of Na^+ channels around threshold potentials make this possibility limited. Therefore, it appears that the I_{toir} activated by depolarization and classical I_{K1} activated by repolarization would play an important role in determining the differential excitability in atrial and ventricular myocytes. In quiescent mammalian cardiac myocytes, classical I_{K1} is considered to provide most of the background conductance, and is responsible for maintaining a polarized membrane resting potential, as well as carrying most of the outward current during the final phase of action potential repolarization [17, 31]. While I_{toir} activated by depolarization [19–21] carries an outward K^+ current with a time course comparable to I_{Na}, would interplay with the rapid I_{Na}, which may play a role in maintaining cell excitability.

The results from present study and previous report [19] showed that density of I_{toir} and classical I_{K1} was less in atrial myocytes, while greater in ventricular myocytes. This may be related to different Kir2.x (Kir2.1, Kir2.2,

and Kir2.3) gene coding in atrium and ventricles. In dog heart, the convincible evidence with multiple approaches including patch clamp recording, Western blotting analysis, cell/tissue immunostaining has demonstrated that different density of I_{K1} in atrium and ventricles is related to heterogeneous expression/subcellular localization of Kir2.1 and Kir2.3. Kir2.1 is predominantly expressed in the ventricle, while Kir2.3 is mainly expressed in the atrium [32]. In addition, it has been found in human hearts that gene and protein expressions of Kir2.1 are less in atrium than those in ventricle, while Kir2.3 is greater in atrium than that in ventricle [33]. Consistent with these reports, our recent studies showed that morphology of human Kir2.3 current stably expressed in HEK 293 cells and the *I–V* relationship curve [34] are similar to I_{K1} recorded in atrial myocytes, whereas that of human Kir2.1 current and *I–V* relationship curve [35] are similar to I_{K1} recorded in ventricular myocytes. Therefore, it is clear that Kir2.1 channel carries a significant I_{toir} during depolarization in ventricular myocytes, which may play a role in maintaining ventricular excitability [20, 21].

The concept of excitability is generally considered to be linked to the availability of Na^+ channels to generate an action potential [12, 36]. However, we [13] and others [37] demonstrated that threshold potential of I_{Na} activation is −65 to −60 mV under conditions of suppressing outward K^+ currents in ventricular cells, which is 10–15 mV less negative than resting membrane potential. The present study showed that the threshold potential of I_{Na} activation was −42 to −46 mV under conditions without blocking outward K^+ current (e.g. I_{toir}), close to the threshold potential (−41 to −48 mV) of action potential activation observed by other groups [38, 39]. Therefore, the threshold potential of action potential and/or I_{Na} activation is 22–30 mV less negative than resting membrane potential, which is probably consisted of the intrinsic passive membrane properties [40] and the active membrane ionic currents including classical I_{K1} [12, 41] and the I_{toir} presented in this and previous studies [18–21] .

I_{toir} carries significant outward current upon the depolarization of action potential over a time course comparable to I_{Na} [18–21]. The threshold potential of I_{toir} activation is more negative (just positive to the E_K) than other time-dependent K^+ currents, such as classical transient outward K^+ current (I_{to}) [42], and ultra-rapid delayed rectifier K^+ current (I_{Kur}) [43]. Therefore, I_{toir} may play a role in the determination of the threshold potential in myocardial cells.

The limitation of the present study is no specific I_{toir} channel blocker available. We therefore used Ba^{2+} as a tool to study the potential physiological role of I_{toir} in maintaining excitability of guinea pig ventricular myocytes, and demonstrated that Ba^{2+} at 5 μmol/L significantly inhibited both I_{toir} and classical I_{K1}, and induced a left-downward shift of the current strength-duration curve under conditions of consistent membrane potential of −80 mV to limit the potential contribution of alteration of resting membrane potential, suggesting I_{toir} indeed plays a role in maintaining cell excitability. Mechanism that I_{toir} inhibition by Ba^{2+} increases cell excitability correlates to the shift of the threshold potential of I_{Na} activation to more negative, and the effect is independent of change in I_{Na}, indicating that I_{toir} determines the threshold potential of action potential generation in guinea pig ventricular myocytes. No information is available in literature about a current responsible for cardiac threshold potential to compare with our observations.

A better understanding of the ionic mechanism governing cardiac ventricular excitability is important for designing improved antiarrhythmic strategies. It is well-known that the abnormal cardiac excitability may cause dangerous ventricular arrhythmias, and increase in excitability may rise to a proarrhythmic precursor state that results in reentrant, automatic and triggered arrhythmias [44]. The present study has provided the direct evidence that I_{toir} inhibition by Ba^{2+} may shift the threshold potential of I_{Na} to more negative, and therefore increases cell excitability. In other words, I_{toir} increase by any intermediate may shift the threshold potential to more positive, and will decrease cardiac excitability, which probably exerts antiarrhythmic effects. Our previous study showed that inactivation process of I_{toir} was strongly dependent on intracellular free Mg^{2+} [20]. Increase of intracellular free Mg^{2+} delays the inactivation of I_{toir} carried by human Kir2.1 channels, enhances, but not decreases, the contribution of the current during depolarization of cardiac action potential [20]. Thus, this may reduce cellular excitability. In cardiac myocytes, the depolarization-activated I_{toir} would contribute significantly to phase 1 repolarization of action potential [18, 19], and therefore may play an important role in maintaining cardiac excitability. In an earlier study, Murphy and colleagues demonstrated that intracellular free Mg^{2+} level significantly elevated (from

1 mmol/L to >2.0 mmol/L) during cardiac ischemia [45]. Therefore, the increase of cytosolic free Mg^{2+} level may actually decrease the excitability by delaying inactivation of I_{toir}, which is clearly a protective effect during myocardial ischemia. It is unknown whether the decreased cardiovascular events by dietary magnesium intake [46–48] would be related to the reduced myocardial excitability via delaying I_{toir} inactivation.

Collectively, we have demonstrated that the excitability is distinctive in atrial and ventricular myocytes of guinea pig heart. The differential excitability is contributed partially by classical I_{K1} and mainly by I_{toir}, while the potential contribution of I_{Na} is limited. Inhibition of I_{toir} by low concentrations of Ba^{2+} significantly increases excitability in ventricular myocytes, indicating that I_{toir} activated by depolarization plays a major role in the early repolarization of action potential and in maintaining ventricular cell excitability. Our study has provided a novel ionic mechanism that controls cardiac excitability, which is potentially important for the understanding of cardiac electrophysiology and the development of novel approaches to manage life-threatening ventricular arrhythmias.

REFERENCES

1 Boyett MR, Jewell BR. Analysis of the effects of changes in rate and rhythm upon electrical activity in the heart. Prog Biophys Mol Biol 1980; 36: 1–52.

2 Bean JW. An attempt to use chronaxie as a measure of excitability. Am J Physiol 1934; 107; 275–328.

3 Geddes LA. Accuracy limitations of chronaxie values. IEEE Tran Biomed Eng 2004; 51: 176–181.

4 Nodera H, Kaji R. Nerve excitability testing and its clinical application to neuromuscular diseases. Clin Neurophysiol 2006; 117: 1902–1916.

5 Gomes PA, de Galvao KM, Mateus EF. Excitability of isolated hearts from rats during postnatal development. J Cardiovasc Electrophysiol 2002; 13: 355–360.

6 Irnich W. The chronaxie time and its practical importance. Pacing Clin Electrophysiol 1980; 3: 292–301.

7 Kay GN, Mulholland DH, Epstein AE, Plumb VJ. Effect of pacing rate on the human atrial strength-duration curve. J Amer Coll Cardiol 1990; 15: 1618–1623.

8 Li GR, Fang DC, Hu CJ, Lu FH. Effects of dauricine on the physiologic properties of myocardium. Acta Acad Med Wuhan 1984; 4: 82–84.

9 Tung L, Sliz N, Mulligan MR. Influence of electrical axis of stimulation on excitation of cardiac muscle cells. Circ Res 1991; 69: 722–730.

10 Hund TJ, Rudy Y. Determinants of excitability in cardiac myocytes: mechanistic investigation of memory effect. Biophys J 2000; 79: 3095–3104.

11 Dhamoon AS, Jalife J. The inward rectifier current (I_{K1}) controls cardiac excitability and is involved in arrhythmogenesis. Heart Rhythm 2005; 2: 316–324.

12 Golod DA, Kumar R, Joyner RW. Determinants of action potential initiation in isolated rabbit atrial and ventricular myocytes. Am J Physiol Heart Circ Physiol 1998; 274: H1902–H1913.

13 Li GR, Lau CP, Shrier A. Heterogeneity of sodium current in atrial vs epicardial ventricular myocytes of adult guinea pig hearts. J Mol Cell Cardiol 2002; 34: 1185–1194.

14 Lopatin AN, Nichols CG. Inward rectifiers in the heart: an update on I(K1). J Mol Cell Cardiol 2001; 33: 625–638.

15 Matsuda H, Saigusa A, Irisawa H. Ohmic conductance through the inwardly rectifying K channel and blocking by internal Mg^{2+}. Nature 1987; 325: 156–159.

16 Noble D. The surprising heart: a review of recent progress in cardiac electrophysiology. J Physiol 1984; 353: 1–50.

17 Shimoni Y, Clark RB, Giles WR. Role of an inwardly rectifying potassium current in rabbit ventricular action potential. J Physiol 1992; 448: 709–727.

18 Li GR, Sun H, Nattel S. Characterization of a transient outward K^+ current with inward rectification in canine ventricular myocytes. Am J Physiol Cell Physiol 1998; 274: C577–C585.

19 Li GR, Yang B, Sun H, Baumgarten CM. Existence of a transient outward K^+ current in guinea pig cardiac myocytes. Am J Physiol Heart CircPhysiol 2000; 279: H130–H138.

20 Zhang DY, Lau CP, Li GR. Human Kir2.1 channel carries a transient outward potassium current with inward rectification. Pflugers Arch 2009; 457: 1275–1285.

21 Li GR, Dong MQ. Revisit of the cardiac inward rectifier potassium current I_{K1}. Open Circ Vasc J 2010; 3: 95–102.

22 Fozzard HA, Schoenberg M. Strength-duration curves in cardiac Purkinje fibres: effects of liminal length and charge distribution. J Physiol 1972; 226: 593–618.

23 Hutter OF, Noble D. Rectifying properties of heart muscle. Nature 1960; 188: 495.

24 Hall AE, Hutter OF, Noble D. Current-voltage relations of Purkinje fibres in sodium-deficient solutions. J Physiol 1963; 166: 225–240.

25 Li GR, Dong MQ. Pharmacology of cardiac potassium channels. Adv Pharmacol 2010; 59: 93–134.

26 DiFrancesco D, Ferroni A, Visentin S. Barium-induced blockade of the inward rectifier in calf Purkinje fibres. Pflugers Arch 1984; 402: 446–453.

27 Delmar M, Glass L, Michaels DC, Jalife J. Ionic basis and analytical solution of the wenckebach phenomenon in guinea

pig ventricular myocytes. Circ Res 1989; 65: 775–788.
28 Kakei M, Noma A, Shibasaki T. Properties of adenosine-triphosphate-regulated potassium channels in guinea-pig ventricular cells. J Physiol 1985; 363: 441–462.
29 Nichols CG, Ripoll C, Lederer WJ. ATP-sensitive potassium channel modulation of the guinea pig ventricular action potential and contraction. Circ Res 1991; 68: 280–287.
30 Jalife J. Inward rectifier potassium channels control rotor frequency in ventricular fibrillation. Heart Rhythm 2009; 6: S44–S48.
31 Nichols CG, Makhina EN, Pearson WL, Sha Q, Lopatin AN. Inward rectification and implications for cardiac excitability. Circ Res 1996; 78: 1–7.
32 Melnyk P, Zhang L, Shrier A, Nattel S. Differential distribution of Kir2.1 and Kir2.3 subunits in canine atrium and ventricle. Am J Physiol Heart Circ Physiol 2002; 283: H1123–H1133.
33 Gaborit N, Le Bouter S, Szuts V, Varro A, Escande D, Nattel S, Demolombe S. Regional and tissue specific transcript signatures of ion channel genes in the non-diseased human heart. J Physiol 2007; 582: 675–693.
34 Zhang DY, Zhang YH, Sun HY, Lau CP, Li GR. Epidermal growth factor receptor tyrosine kinase regulates the human inward rectifier potassium K(IR)2.3 channel, stably expressed in HEK 293 cells. Br J Pharmacol 2011; 164: 1469–1478.
35 Zhang DY, Wu W, Deng XL, Lau CP, Li GR. Genistein and tyrphostin AG556 inhibit inwardly-rectifying Kir2.1 channels expressed in HEK 293 cells via protein tyrosine kinase inhibition. Biochim Biophys Acta 2011; 1808: 1993–1999.
36 Joyner RW, Ramza BM, Osaka T, Tan RC. Cellular mechanisms of delayed recovery of excitability in ventricular tissue. Am J Physiol Heart Circ Physiol 1991; 260: H225–H233.
37 Pu J, Boyden PA. Alterations of Na^+ currents in myocytes from epicardial border zone of the infarcted heart. A possible ionic mechanism for reduced excitability and postrepolarization refractoriness. Circ Res 1997; 81: 110–119.
38 Firek L, Giles WR. Electrophysiological analyses of threshold conditions and rate-dependent failure of excitation in single myocytes from rabbit ventricle. Can J Cardiol 1997; 13: 1113–1124.
39 Ramza BM, Tan RC, Osaka T, Joyner RW. Cellular mechanism of the functional refractory period in ventricular muscle. Circ Res 1990; 66: 147–162.
40 Arnsdorf MF. Membrane factors in arrhythmogenesis: concepts and definitions. Prog Cardiovasc Dis 1977; 19: 413–429.
41 Ibarra J, Morley GE, Delmar M. Dynamics of the inward rectifier K^+ current during the action potential of guinea pig ventricular myocytes. Biophys J 1991; 60: 1534–1539.
42 Li GR, Feng J, Wang Z, Fermini B, Nattel S. Comparative mechanisms of 4-aminopyridine-resistant *I*to in human and rabbit atrial myocytes. Am J Physiol Heart Circ Physiol 1995; 269: H463–H472.
43 Yue L, Feng J, Li GR, Nattel S. Characterization of an ultrarapid delayed rectifier potassium channel involved in canine atrial repolarization. J Physiol 1996; 496: 647–662.
44 Arnsdorf MF. Cardiac excitability, the electrophysiologic matrix and electrically induced ventricular arrhythmias: order and reproducibility in seeming electrophysiologic chaos. J Am Coll Cardiol 1991; 17: 139–142.
45 Murphy E, Steenbergen C, Levy LA, Raju B, London RE. Cytosolic free magnesium levels in ischemic rat heart. J Biol Chem 1989; 264: 5622–5627.
46 Volpe SL. Magnesium in disease prevention and overall health. Adv Nutr 2013; 4: 378S–383S.
47 Chiuve SE, Sun Q, Curhan GC, Taylor EN, Spiegelman D, Willett WC, Manson JE, Rexrode KM, Albert CM. Dietary and plasma magnesium and risk of coronary heart disease among women. J Am Heart Assoc 2013; 2: e000114.
48 Del Gobbo LC, Imamura F, Wu JH, de Oliveira Otto MC, Chiuve SE, Mozaffarian D. Circulating and dietary magnesium and risk of cardiovascular disease: a systematic review and meta-analysis of prospective studies. Am J Clin Nutr 2013; 98: 160–173.